LSDetector: An Open-Source Tool Bridging Landslide Detection Models and Real-World Deployment through Three-Stage Transfer Learning

Zijin Fu[1,2], Fawu Wang[1,*], Sansar Raj Meena[2], Senlin Luo[1,2], Zihan Tu[1], Filippo Catani[2]

[1] College of Civil Engineering, Tongji University, Shanghai 200092, China

[2] Department of Geosciences, University of Padova, Padova 35129, Italy

[*] Corresponding author. E-mail: wangfw@tongji.edu.cn

Project home page: github.com/klaus2023/LSDetector

This manuscript is a non-peer-reviewed preprint submitted to EarthArXiv.

Abstract

Rapid and reusable landslide detection from remote-sensing imagery remains challenging because practical deployment often requires cross-region transfer learning, limited local labels, and reproducible model-to-product workflows. This paper presents LSDetector, an open-source local workbench that bridges advanced landslide detection models and real-world deployment through three-stage transfer learning. The platform integrates LSDFormer and LSDSAM model families, registry-based management of model weights and datasets, and a workflow consisting of task-adaptive fine-tuning, domain-adversarial fine-tuning, and target-specific fine-tuning. Using the Wuping rainfall-triggered landslide area as a demonstration case, we evaluate model adaptation behavior, computational efficiency, and large-area deployment performance. Benchmark experiments show that LSDSAM-H achieves the best overall performance among the tested models, while LSDFormer provides the lightest and fastest deployment option. In practical mapping, LSDSAM-H was used to support two rounds of AI-assisted refinement and full-area inference over PlanetScope imagery covering 17,295 km^2, producing 40,400 candidate landslide polygons. These results demonstrate that LSDetector can reduce manual annotation effort and support semi-automatic construction of reviewable regional landslide inventories.

Keywords

Landslide detection, remote sensing, deep learning, foundation model

Introduction

Landslides are among the most destructive geological hazards worldwide, particularly in mountainous regions. Under the combined influence of climate change and the frequent occurrence of major earthquakes, their impacts on human life and property have become increasingly severe (Alcántara-Ayala 2025). Following extreme rainfall or strong seismic events, tens of thousands or even hundreds of thousands of landslides may be triggered across an affected area (Gariano and Guzzetti 2016; Tanyaş et al. 2017). In regions with highly complex predisposing conditions, landslide occurrence often shows considerable spatial variability and uncertainty. In this context,

landslide detection (LSD) aims to derive landslide inventories from remote sensing images and serves as a fundamental task for disaster prevention, risk reduction and scientific research.

Methods for LSD can generally be grouped into two categories: manual visual interpretation and automated approaches. Automated methods can substantially reduce the cost of manual annotation and are gradually becoming the dominant paradigm as earth observation data continue to expand and the demand for LSD applications keeps increasing. Over the past few decades, automated LSD methods have evolved through several stages, moving from feature engineering (Chen et al. 2018) to classical machine learning (Gariano and Guzzetti 2016) to deep learning (Fu et al. 2026b; Wu et al. 2024), and to foundation models (Fu et al. 2026a). AI-based methods are gradually becoming the mainstream for LSD. Many recent studies have developed their models around several key directions, including multi-level feature fusion (Xu et al. 2022), attention mechanisms (Ji et al. 2020), multi-modal fusion (Yang et al. 2025) and lightweight design (Dong et al. 2024).

Although landslide detection models have continued to evolve, AI-centered LSD tools that can be reused across different regions remain limited. Most existing studies still follow a model-oriented experimental paradigm, in which a model is developed and evaluated on training and testing sets from a single study area or dataset (Fu et al. 2026b). This paradigm often provides limited support for practical reuse, cross-region transfer and deployment under scarce-label conditions. Developing a reusable AI tool for landslide detection involves coupled challenges related to model design, data availability and training strategy. Recent advances in foundation models, the growing availability of landslide detection datasets (Xu et al. 2024) and the emergence of diverse transfer learning strategies (Fu et al. 2026a) have created new opportunities to address these challenges from complementary perspectives. Together, these developments provide a broader set of deployable options for adapting AI-based LSD methods to different regions, data conditions and application scenarios.

To address the challenges of LSD in unseen areas, we propose LSDetector, an integrated management platform that brings models, datasets and deployment strategies into a unified AI-based LSD workflow. Specifically, LSDetector incorporates two state-of-the-art models for LSD, namely LSDFormer and LSDSAM (Fu et al. 2026a,b), and implements a deployment framework based on a three-stage transfer learning paradigm, including task-adaptive fine-tuning (TAFT), domain-adversarial fine-tuning (DAFT) and target-specific fine-tuning (TSFT). The associated models, network weights and datasets are organized through registry-based management. To support practical deployment, the platform further provides visual interfaces for configuring key hyperparameters during the three-stage transfer learning process. These components are integrated into a concise and user-friendly graphical interface, allowing users to apply AI-assisted LSD workflows under few-shot conditions with reduced technical barriers. We demonstrate the platform in the Wuping rainfall-triggered landslide area to assess benchmark adaptation, model efficiency, and large-area deployment.

Data

Source domain datasets

Landslide77K is used as the source-domain dataset to introduce landslide-specific prior knowledge during transfer learning. It was assembled from several public landslide datasets, including LMHLD (Liu et al. 2025), CAS (Xu et al. 2024), GDCLD (Fang et al. 2024), HRGLDD (Meena et al. 2023), GVLM (Zhang et al. 2023), Landslide4Sense (Ghorbanzadeh et al. 2022), the Bijie dataset (Ji et al. 2020), the RLZX (Fu et al. 2025) and ELNT datasets (Fu et al. 2026b). It contains more than 77,000 image-mask samples. The dataset covers diverse regions, sensors, spatial resolutions, landslide types, and triggering conditions. As one of the few pretraining datasets in LSD field, it provides a strong basis for improving the generalization of different LSD models.

Demonstration area

The LSDetector demonstration area is located in the mountainous region near the Fujian–Guangdong–Jiangxi border in southeastern China, where intense rainfall in June 2024 triggered clustered landslides (Luo et al. 2026). The region is characterized by steep and dissected terrain, weathered bedrock, dense drainage networks, subtropical monsoon rainfall, and frequent human disturbance along roads and settlements. These conditions produce heterogeneous post-disaster surface patterns, with landslide scars varying in size, exposure, morphology, and visibility across complex terrain and land-cover settings. The post-disaster PlanetScope images within three months after the rainfall event were collected, providing temporally denser observations and clearer cloud-free and shadow-free coverage of the affected area as data input for LSDetector.

Design and implementation

Overview and pipeline architecture

LSDetector is designed as a local AI-assisted workbench for regional landslide detection, integrating model selection, model-weight management, dataset registration, adaptive fine-tuning, deployment inference, evaluation and GIS-compatible export within a unified software environment, as shown in Fig. 1. The platform is organized around three repositories: a model repository for LSDFormer and LSDSAM variants, a weight repository for TAFT, DAFT, TSFT and inference-ready model weights, and a dataset repository for source-domain, target-domain, locally annotated and evaluation datasets. This registry-based organization enables different models, weights and datasets to be selected and reused within the same deployment workflow.

In the current implementation, TAFT process is not provided as a routine user-side training module because it requires large-scale supervised training and substantial computational resources. Instead, LSDetector offers TAFT model weights trained on Landslide77K as deployable starting points. Users can then perform DAFT to reduce target-domain distribution shifts using unlabeled regional imagery, followed by TSFT to incorporate local annotations or corrected outputs when available. After adaptation, the inference module generates probability rasters, binary masks and landslide polygons through tile preparation, patch prediction, mosaicking and vectorization. These outputs can be exported as GIS-compatible products for quantitative assessment, map-based inspection and manual editing in external GIS software such as ArcGIS, ArcGIS Pro and QGIS.

Detection models

LSDetector currently integrates two complementary LSD model families, namely LSDFormer and LSDSAM, which serve as the core AI engines of the platform. This design provides users with a flexible model selection mechanism rather than a fixed single-model setting. Different backbones can be selected according to available hardware resources, expected inference speed and accuracy requirements. In particular, LSDFormer supports efficient deployment with a lightweight architecture, while the LSDSAM series provides three backbone scales, including base, large and huge, to accommodate different levels of computational capacity and detection demand.

LSDFormer was originally developed as an efficient CNN-Transformer hybrid network for cross-region landslide detection by transfer learning (Fu et al. 2026b). It follows a compact encoder-decoder design and combines convolutional inductive bias with Transformer-based global context modeling. This structure allows the model to capture both local landslide boundaries and broader spatial dependencies while maintaining relatively low computational cost. In LSDetector, LSDFormer is used as an efficient deep segmentation model for rapid deployment, especially when users require a lightweight model with stable cross-region performance.

LSDSAM represents the foundation-model-based branch of LSDetector. It was developed by adapting the Segment Anything Model (SAM) to landslide detection through enhanced transfer learning (Fu et al. 2026a). Instead of training a segmentation model entirely from scratch, LSDSAM leverages the

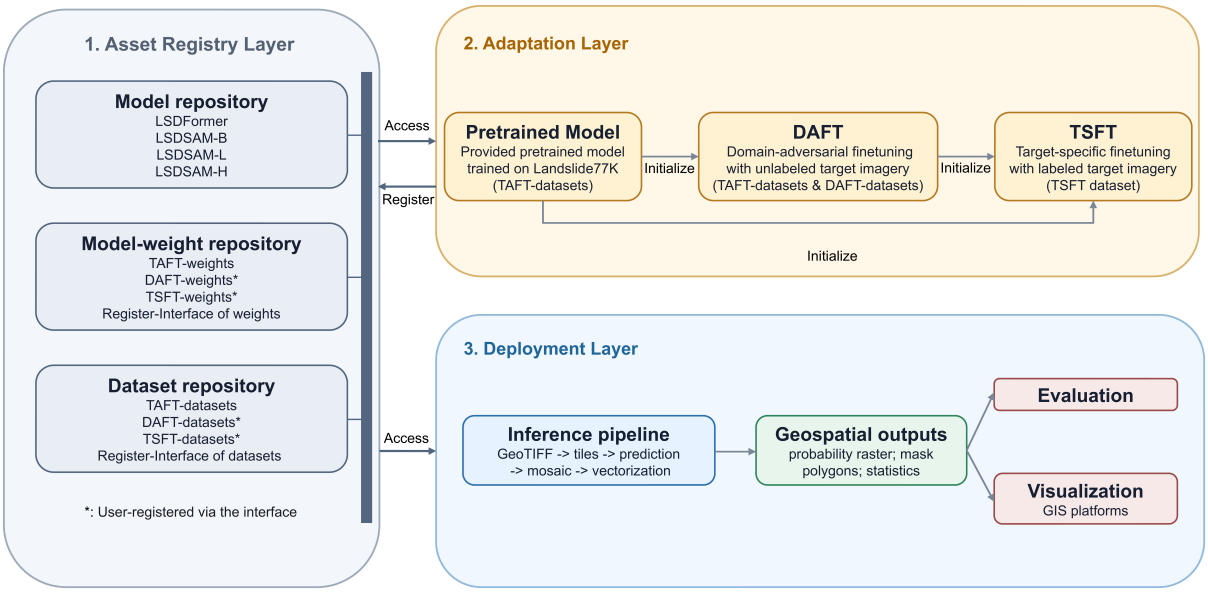

Fig. 1 Architecture of LSDetector.

visual representation capability of SAM and introduces landslide-specific adaptation components to improve boundary delineation and few-shot transferability. In the current implementation, LSDetector incorporates three LSDSAM variants, corresponding to the base, large and huge SAM backbones. These variants provide different trade-offs between computational cost, model capacity and detection accuracy, allowing users to choose a suitable version for different deployment conditions.

Three-stage transfer learning

LSDetector implements a staged adaptation workflow derived from the transfer learning strategy of LSDSAM (Fu et al. 2026a), and generalizes it to the LSDFormer and LSDSAM model families embedded in the platform. As illustrated in Fig. 2, the workflow consists of three successive operations: task-adaptive fine-tuning, domain-adversarial fine-tuning and target-specific fine-tuning. TAFT builds the initial landslide-aware representation, DAFT adjusts this representation to the visual distribution of a new deployment area, and TSFT incorporates limited local supervision to refine the final mapping behavior. By packaging these operations into an interactive platform, LSDetector turns a technically demanding adaptation process into a configurable deployment workflow. This differs from conventional LSD experiments that usually end with offline model evaluation; here, the model can be iteratively improved with only a small amount of local annotation, allowing AI to support practical landslide mapping while reducing the burden of manual labeling.

In TAFT, globally distributed landslide samples are used to expose the model to diverse landslide appearances before it is applied to a target region. This stage helps LSDFormer and LSDSAM acquire task-oriented visual responses related to landslide scars, boundaries, texture and background context. DAFT then introduces target-domain imagery into the adaptation process. Through adversarial domain adaptation, the model is guided to retain landslide-relevant responses while suppressing appearance bias caused by differences in sensor type, resolution, illumination, land cover and geomorphic background. TSFT is the final local calibration step, where a small set of user-provided labels or corrected previous outputs is used to adapt the model to the landslide-specific visual characteristics of the target area. In this way, LSDetector supports a gradual path from global landslide knowledge to target-area few-shot refinement and final deployment.

Constructing procedure of landslide inventory

In practical use, LSDetector follows a registry-driven workflow for constructing a regional

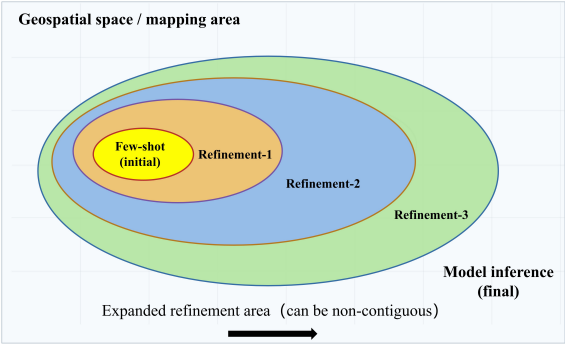

Fig. 2 AI-assisted iterative refinement workflow.

landslide inventory. Users first register the required assets, including the target-domain imagery and available local landslide labels, and then select an appropriate LSD model, pretrained weights and adaptation stage according to data availability and local labeling conditions. The selected model can be adapted by DAFT using unlabeled target imagery and further calibrated by TSFT when local annotations or corrected samples are available. After adaptation, the deployment pipeline produces probability rasters, binary masks and vectorized landslide polygons, which are exported as GIS-compatible geospatial products for inspection and editing in external GIS software such as ArcGIS, ArcGIS Pro and QGIS. Based on these outputs, LSDetector supports an iterative model-assisted inventory refinement procedure, as shown in Fig. 2. The process starts from a limited number of manually annotated samples, which are used to obtain an initial target-specific model. The model is then applied to a larger area, and users refine the predicted polygons in external GIS software by correcting false positives, adding missed landslides and retaining reliable predictions. The corrected results are registered as an updated TSFT dataset and merged with previous local samples for the next round of fine-tuning and inference. By repeating this cycle over progressively expanded areas, the landslide inventory can be improved from sparse initial labels to a more complete and reviewable regional mapping product, while substantially reducing the need for fully manual annotation.

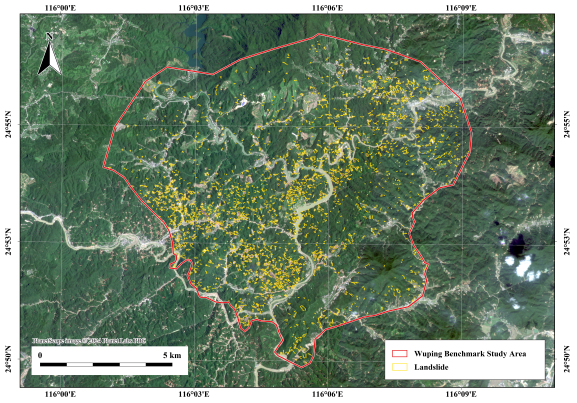

Fig. 3 Wuping benchmark dataset.

Table 1 Performance comparison under 0-shot and 8-shot settings on Wuping, measured by mIoU (%).

Model	0-shot		8-shot	
	w/o DAFT	with DAFT	w/o DAFT	with DAFT
LSDFormer	47.7	52.9±0.8	59.1	60.7±1.1
LSDSAM-B	49.7	50.6±2.1	58.7	56.2±2.9
LSDSAM-L	49.6	49.1±1.0	58.4	53.4±4.0
LSDSAM-H	52.8	49.7±1.5	61.4	52.1±3.0

Results and discussion

Wuping benchmark evaluation

The experimental benchmark was conducted in the Wuping study area shown in Fig. 3. A total of 2,530 landslide polygons were carefully annotated within the benchmark area shown in the figure. These annotations were registered in LSDetector as 151 non-overlapping 256 × 256 image-label patches and were split at a 7:3 ratio into 106 training patches and 45 evaluation patches.

Table 1 evaluates whether DAFT should be used before local adaptation, comparing TAFT-only and DAFT-initialized weights under both 0-shot inference and an 8-shot initial TSFT setting. Because adversarial alignment and few-shot optimization are sensitive to stochastic initialization, sample composition, and checkpoint selection, we repeated the experiment ten times to obtain more stable estimates. The results show a clear DAFT benefit for LSDFormer, especially in the 0-shot setting, and a smaller positive effect for LSDSAM-B. By contrast, LSDSAM-L and LSDSAM-H exhibit negative transfer after DAFT, particularly under 8-shot TSFT. A plausible explanation is that

Table 2 Performance statistics over ten random 7:3 Wuping splits, measured by five evaluation metrics (%).

Model	IoU	mIoU	F1	Precision	Recall
LSDFormer	34.7 ± 1.2	65.4 ± 0.6	51.6 ± 1.4	59.0 ± 4.2	46.1 ± 3.6
LSDSAM-B	35.4 ± 1.3	65.7 ± 0.7	52.3 ± 1.4	58.1 ± 4.0	47.8 ± 2.8
LSDSAM-L	35.5 ± 1.4	65.8 ± 0.8	52.4 ± 1.5	59.3 ± 3.2	47.2 ± 3.0
LSDSAM-H	37.5 ± 0.8	66.9 ± 0.4	54.5 ± 0.9	61.5 ± 4.1	49.2 ± 1.7

Table 3 Model complexity and practical inference efficiency of the registered LSDetector models.

Model	Input	Total params (M)	Trainable params (M)	FLOPs (G)	Training GPU memory (GB)	Inference speed (FPS)	Deployment speed (km^2/s)
LSDFormer	256×256	37.7	7.9	19.6	1.0~2.9	46.4	4.8
LSDSAM-B	512×512	110.1	13.5	261.6	2.6~8.4	26.1	2.9
LSDSAM-L	512×512	339.5	17.4	840.3	5.3~16.3	18.6	2.1
LSDSAM-H	512×512	680.9	21.6	1704.4	8.4~25.0	11.2	1.6

the LSDSAM family already inherits strong generic representations from the SAM backbone, and this robustness increases with backbone scale; forcing additional domain alignment on a narrow target domain can therefore distort transferable features rather than improve them. Table 2 further reduces split-induced uncertainty by evaluating the four models over ten random 7:3 splits using common semantic-segmentation metrics, including foreground IoU, mIoU, F1, precision, and recall. Across these statistics, performance increases from LSDFormer to LSDSAM-B, LSDSAM-L, and LSDSAM-H, consistent with the increasing parameter capacity and the corresponding rise in training and inference cost.

Model complexity analysis

Table 3 summarizes the computational complexity of the four registered models in LSDetector. Total parameters denote all weights in the loaded TAFT inference model, while trainable parameters indicate the subset updated during TSFT under the LoRA configuration. FLOPs were estimated for one input patch using the model-specific default size, namely 256×256 for LSDFormer and 512×512 for LSDSAM. Training GPU memory is measured as the net peak memory of a TSFT training step, and is reported as the interval from batch size 1 to 4. Inference speed refers to direct forward prediction on preprocessed patches, whereas deployment speed measures the complete LSDetector patch-based inference pipeline over valid Wuping GeoTIFF pixels from PlanetScope images, with a patch size of 256 and a stride of 128. The results show that LSDFormer is the lightest and fastest option, while LSDSAM scales from B to H with increasing parameters, FLOPs, and training memory, providing higher-capacity alternatives when hardware resources allow.

Practical deployment on the Wuping area

To demonstrate the practical deployment capability of LSDetector beyond benchmark evaluation, we applied LSDSAM-H to a large-area landslide mapping task in Wuping. The experiment strictly followed the three-stage transfer-learning and iterative refinement workflow shown in Fig. 2. Starting from the few-shot stage, the model-assisted inventory construction was expanded through two refinement rounds (Fig. 4). In refinement-1 and refinement-2, LSDSAM-H supported semi-automatic delineation and refinement of 2,530 and 6,200 landslide polygons, respectively, which were then used to improve the target-specific mapping process. The final deployment covered 17,295 km^2 of PlanetScope imagery in the Wuping region and produced 40,400 candidate landslide polygons over the full mapping extent. The eight randomly selected out-of-sample subregions in Fig. 4 illustrate that LSDSAM-H can still delineate dense landslide clusters on unseen areas with complex roads, vegetation and mountainous backgrounds. These products should not be

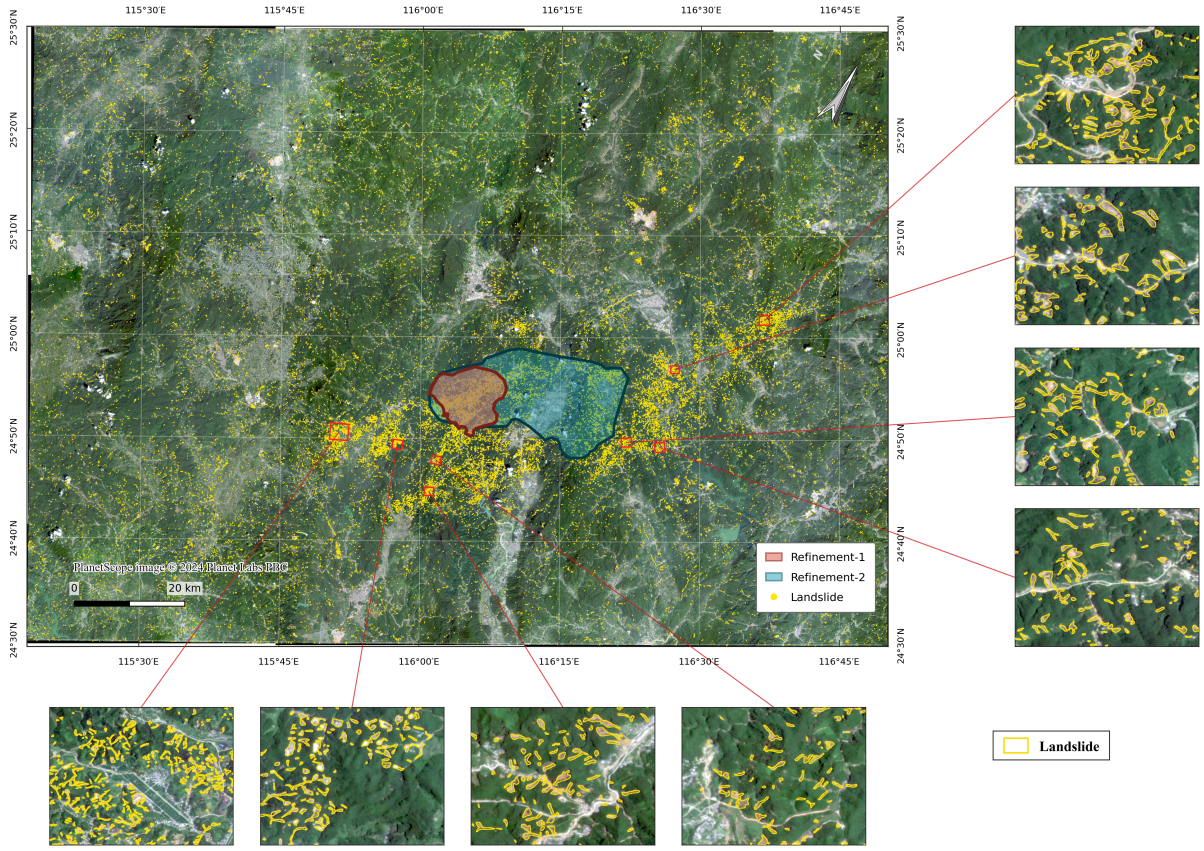

Fig. 4 Practical deployment of LSDSAM-H in the Wuping area through iterative AI-assisted refinement.

regarded as a fully verified inventory; further manual checking, or additional iterative refinement rounds, is still required. Nevertheless, the experiment demonstrates that LSDetector can substantially reduce manual annotation workload and promote semi-automatic extraction of large-area landslide inventories from remote-sensing imagery.

Prospects and limitations

The main advantage of LSDetector is that it turns advanced cross-region landslide detection models into a practical local workflow. Built on transferable landslide knowledge from large source-domain datasets and foundation-model representations, it supports model deployment in new regions with limited local annotation, reducing manual labeling costs while maintaining reliable detection performance. The software further integrates model weights, datasets, adaptation modules, inference, evaluation, GIS-compatible export and externally corrected refinement records, allowing users without extensive AI experience to conduct reproducible landslide mapping and model adaptation locally.

Current limitations mainly arise from the RGB-based design of the embedded models. Optical imagery is vulnerable to clouds, vegetation cover, terrain shadows, and complex illumination, especially in mountainous regions. Future versions of LSDetector should therefore incorporate SAR, high-resolution terrain data, and other geospatial variables to improve robustness. The TAFT data repository should also be expanded in scale and diversity, with LSDetector serving as a data engine for accumulating predictions, expert corrections, and new samples. Another promising direction is dynamic landslide inventorying, where time-series models infer not only landslide locations but also occurrence timing from multi-temporal remote sensing data.

Conclusion

This study introduced LSDetector as a practical software bridge between landslide detection model research and operational remote-sensing deployment. By integrating LSDFormer, LS-

DSAM, model-weight and dataset repositories, and a configurable TAFT-DAFT-TSFT workflow, the platform converts isolated model weights into reusable regional mapping procedures. The Wuping experiments show that the embedded model family provides complementary choices: LSDFormer offers efficient lightweight deployment, whereas LSDSAM-H provides the strongest segmentation performance in the benchmark tests. The practical deployment further demonstrates the value of LSDetector for large-area landslide inventory construction, where LSDSAM-H supported iterative refinement and produced 40,400 candidate polygons over 17,295 km^2 of PlanetScope imagery. Although the generated inventory still requires expert verification and possible additional refinement rounds, the workflow substantially reduces the burden of fully manual interpretation and provides a reproducible path for AI-assisted landslide mapping. Future development should extend LSDetector toward multimodal inputs, larger and more diverse source-domain datasets, and dynamic time-series landslide inventorying.

Acknowledgments

This work was supported by the National Science Foundation of China (Grant No. 42230715 and No. W2511039).

References

Alcántara-Ayala, I. (2025). "Landslides in a Changing World". In: *Landslides* 22.9, pp. 2851–2865.

Chen, F., Yu, B., & Li, B. (2018). "A Practical Trial of Landslide Detection from Single-Temporal Landsat8 Images Using Contour-Based Proposals and Random Forest: A Case Study of National Nepal". In: *Landslides* 15.3, pp. 453–464.

Dong, A., Dou, J., Li, C., et al. (2024). "Accelerating Cross-Scene Co-Seismic Landslide Detection Through Progressive Transfer Learning and Lightweight Deep Learning Strategies". In: *IEEE Transactions on Geoscience and Remote Sensing* 62, pp. 1–13.

Fang, C., Fan, X., Wang, X., et al. (2024). "A Globally Distributed Dataset of Coseismic Landslide Mapping via Multi-Source High-Resolution Remote Sensing Images". In: *Earth System Science Data Discussions*, pp. 1–42.

Fu, Z., Wang, F., Ma, H., et al. (2025). "Records of Shallow Landslides Triggered by Extreme Rainfall in July 2024 in Zixing, China". In: *Scientific Data* 12.1, p. 1364.

Fu, Z., Wang, F., Tu, Z., et al. (2026a). "LSDSAM: Harnessing Visual Foundation Model and Enhanced Transfer Learning Towards Practical Landslide Detection in Few-shot Scenarios". In: *IEEE Journal of Selected Topics in Applied Earth Observations and Remote Sensing*.

Fu, Z., Wang, F., Zhong, J., et al. (2026b). "A CNN–Transformer Hybrid Network for Efficient Cross-Region Landslide Detection by Transfer Learning". In: *Landslides*.

Gariano, S. L., & Guzzetti, F. (2016). "Landslides in a Changing Climate". In: *Earth-Science Reviews* 162, pp. 227–252.

Ghorbanzadeh, O., Xu, Y., Ghamisi, P., et al. (2022). "Landslide4Sense: Reference Benchmark Data and Deep Learning Models for Landslide Detection". In: *IEEE Transactions on Geoscience and Remote Sensing* 60, pp. 1–17.

Ji, S., Yu, D., Shen, C., et al. (2020). "Landslide Detection from an Open Satellite Imagery and Digital Elevation Model Dataset Using Attention Boosted Convolutional Neural Networks". In: *Landslides* 17.6, pp. 1337–1352.

Liu, G., Wang, Y., Chen, X., et al. (2025). "LMHLD: A Large-Scale Multisource High-Resolution Landslide Dataset for Landslide Detection Based on Deep Learning". In: *IEEE Transactions on Geoscience and Remote Sensing* 63, pp. 1–15.

Luo, S., Mao, W., Yang, Z., et al. (2026). "CNXT-Ti-LT–Based Multi-Scale Feature–Aware Susceptibility Mapping of Rainfall-Induced Clustered Landslides in Southeast China". In: *Journal of Geophysical Research: Machine Learning and Computation* 3.2, e2025JH001115.

Meena, S. R., Nava, L., Bhuyan, K., et al. (2023). "HR-GLDD: A Globally Distributed Dataset Using Generalized Deep Learning (DL) for Rapid Landslide Mapping on High-Resolution (HR) Satellite Imagery". In: *Earth System Science Data* 15.7, pp. 3283–3298.

Tanyaş, H., van Westen, C. J., Allstadt, K. E., et al. (2017). "Presentation and Analysis of a Worldwide Database of Earthquake-Induced Landslide Inventories". In: *Journal of Geophysical Research: Earth Surface* 122.10, pp. 1991–2015.

Wu, L., Liu, R., Ju, N., et al. (2024). "Landslide Mapping Based on a Hybrid CNN-transformer Network and Deep Transfer Learning Using Remote Sensing Images with Topographic and Spectral Features". In: *International Journal of Applied Earth Observation and Geoinformation* 126, p. 103612.

Xu, Q., Ouyang, C., Jiang, T., et al. (2022). "MFFENet and ADANet: A Robust Deep Transfer Learning Method and Its Application in High Precision and Fast Cross-Scene Recognition of Earthquake-Induced Landslides". In: *Landslides* 19.7, pp. 1617–1647.

Xu, Y., Ouyang, C., Xu, Q., et al. (2024). "CAS Landslide Dataset: A Large-Scale and Multisensor Dataset for Deep Learning-Based Landslide Detection". In: *Scientific Data* 11.1, p. 12.

Yang, C., Zhu, Y., Zhang, J., et al. (2025). "A Feature Fusion Method on Landslide Identification in Remote Sensing with Segment Anything Model". In: *Landslides* 22.2, pp. 471–483.

Zhang, X., Yu, W., Pun, M.-O., et al. (2023). "Cross-Domain Landslide Mapping from Large-Scale Remote Sensing Images Using Prototype-Guided Domain-Aware Progressive Representation Learning". In: *ISPRS Journal of Photogrammetry and Remote Sensing* 197, pp. 1–17.

Zijin Fu
[1] College of Civil Engineering, Tongji University, Shanghai 200092, China
[2] Department of Geosciences, University of Padova, Padova 35129, Italy

Fawu Wang
[1] College of Civil Engineering, Tongji University, Shanghai 200092, China
E-mail: wangfw@tongji.edu.cn

Sansar Raj Meena
[2] Department of Geosciences, University of Padova, Padova 35129, Italy

Senlin Luo
[1] College of Civil Engineering, Tongji University, Shanghai 200092, China
[2] Department of Geosciences, University of Padova, Padova 35129, Italy

Zihan Tu
[1] College of Civil Engineering, Tongji University, Shanghai 200092, China

Filippo Catani
[2] Department of Geosciences, University of Padova, Padova 35129, Italy